HHS Public Access

Author manuscript

Biochem J. Author manuscript; available in PMC 2017 July 15.

Published in final edited form as:

Biochem J. 2016 July 15; 473(14): 2165–2177. doi:10.1042/BCJ20160289.

Catalytic and substrate promiscuity: Distinct multiple chemistries catalyzed by the phosphatase domain of receptor protein tyrosine phosphatase

Bharath Srinivasan[a], **Hanna Marks**[a], **Sreyoshi Mitra**[a], **David M. Smalley**[b], and **Jeffrey Skolnick**[a,c]

[a]Center for the Study of Systems Biology, School of Biology, Georgia Institute of Technology, 950, Atlantic Drive, Atlanta, Georgia 30332, United States

[b]Systems Mass Spectrometry Core (SyMS-C), Georgia Institute of Technology, 950 Atlantic Drive, Atlanta, Georgia 30318, United States

Abstract

The presence of latent activities in enzymes is posited to underlie the natural evolution of new catalytic functions. However, the prevalence and extent of such substrate and catalytic ambiguity in evolved enzymes is difficult to address experimentally given the order-of-magnitude difference in the activities for native and, sometimes, promiscuous substrate/s. Further, such latent functions are of special interest when the activities concerned do not fall into the domain of substrate promiscuity. Here, we show a special case of such latent enzyme activity by demonstrating the presence of two mechanistically distinct reactions catalyzed by the catalytic domain of receptor protein tyrosine phosphatase isoform delta (PTPRδ). The primary catalytic activity involves the hydrolysis of a phosphomonoester bond (C-O-P) with high catalytic efficiency, while the secondary activity is the hydrolysis of a glycosidic bond (C-O-C) with poorer catalytic efficiency. This enzyme also displays substrate promiscuity by hydrolyzing diester bonds while being highly discriminative for its monoester substrates. To confirm these activities, we also demonstrated their presence on the catalytic domain of PTPRΩ, a homologue of PTPRδ. Studies on the rate, metal-ion dependence, pH dependence and inhibition of the respective activities showed that they are markedly different. This is the first study that demonstrates a novel sugar hydrolase and diesterase activity for the phosphatase domain of PTPRδ and PTPRΩ. This work has significant implications for both understanding the evolution of enzymatic activity and the possible physiological role of

[c]Corresponding author, skolnick@gatech.edu, Tel: (404) 407-8975, Fax: (404) 385-7478.

Declaration of interest:

The authors declare no competing interests.

Author contribution statement

BS conceived of the study, participated in its design, carried out the experiments, analyzed and interpreted the results, and drafted the manuscript. HM, SM and DS carried out the experiments. JS conceived of the study, participated in its design and coordination, provided appropriate resources, helped analyze the data, and was involved in drafting and critically reviewing the manuscript. All authors read and approved the final manuscript.

Supporting information

Supporting information contains Table S1 and Fig S1. Sequence and structural identity between PD-PTPRδ and PD-PTPRΩ; Concentration dependence of sugar hydrolysis for PD-PTPRδ; Test of peptide bond hydrolysis for PD-PTPRδ. Fig S2. Inhibition, substrate and metal-ion preference of PD-PTPRδ and PD-PTPRΩ. Fig S3. pNPP and bis-pNPP analogues. Fig S4. PD-PTPRδ and PD-PTPRΩ inhibition across the sugar-hydrolase and phosphatase activities.

this new chemistry. Our findings suggest that the genome might harbor a wealth of such alternative latent enzyme activities in the same protein domain that renders our knowledge of metabolic networks incomplete.

Keywords

catalytic promiscuity; substrate promiscuity; protein tyrosine phosphatase; glycosidic bond; phosphoester bond

Introduction

Numerous studies have demonstrated and discussed the evolutionary implications of catalytic promiscuity and the degeneracy of substrate preferences by enzymes (1–4). Jensen proposed that modern day enzymes, often assumed to be highly specialized for the reactions that they catalyze, have evolved from broad specificity ancestors (5). Further, instances of promiscuity have been extensively reported from members belonging to the haloacid dehalogenase superfamily (1, 6), thioesterases from the hotdog fold superfamily (1) and others (7, 8). Demonstration of the limited number of distinct ligand binding pockets and the emergence of catalytic pockets in proteins without selection for function has further strengthened the understanding that promiscuity and catalysis are inherent features of proteins and that it is very likely (and certainly not surprising) that the tremendous rate accelerations that we see with present day enzymes results from evolutionary selection from a significant random background (9, 10). However, it has been pointed out that most of these promiscuous secondary activities emerge from the same pocket with nature utilizing the same microenvironment optimized to enhance catalytic potential (2). There are very few previous studies that have attempted to characterize activities that are mechanistically distinct and, possibly, emerge from distinct pockets on the protein's surface. The reason for this paucity stems from both technical limitations (different assay systems and possible order-of-magnitude differences in the rates of the primary and the secondary activities) and the lack of a rational framework to search for such secondary activities. In this paper, motivated by our computational work which strongly suggests that the likelihood of finding low level secondary enzymatic function is high, we demonstrate that the phosphatase domain of receptor protein tyrosine phosphatases catalyzes the hydrolysis of glycosidic (COC) bonds apart from its primary activity of cleaving phosphomonoester (COP) bond. This is important because the hydrolysis of COC bond in β-galactosides and COP bond in phosphomonoesters require different functional groups and different mechanism of cleavage (11, 12).

Receptor protein tyrosine phosphatases (PTPRs) are a family of cell surface receptor proteins that antagonize tyrosine kinase signaling. The phosphatase domain of PTPRs catalyze a two-step phosphate monoester hydrolysis reaction through a highly conserved sequence motif (H/V)CX_5R(S/T) with a nucleophilic cysteine. Receptor protein tyrosine phosphatase subtype δ has a cell adhesion extracellular domain and two cytoplasmic protein tyrosine phosphatase (PTP) domains (13, 14). PTPRδ is predominantly expressed in the brain and is known to be involved in the guidance and termination of motor neurons during

embryonic development (15, 16). PTPRδ knockout mice exhibit impaired learning and memory, also indicating that PTPRδ is essential for the organization of neural circuits (17). The above observations, coupled with the knowledge that PTPRσ is a chondroitin sulfate (CS) receptor that propagates chrondritin sulfate proteoglycan (CSPG)-mediated inhibition and heparin sulfate proteoglycan (HSPG)-mediated axon outgrowth (18) and shares almost 77 % sequence identity with PTPRδ, makes one speculate that the role the two PTPRs exert in neuronal growth might be inextricably interlinked with recognition and processing of sugar moieties alongside phosphate moieties.

In this paper, we report a novel sugar hydrolase activity in the phosphatase domain (PD) of PTPRδ. Furthermore, the enzyme also displays substrate promiscuity by hydrolyzing the diester bond while showing a high-level of discrimination in its primary monoesterase substrate preference. Compared to its primary phosphatase activity, the newly identified sugar hydrolase activity shows marked differences vis-à-vis rate enhancement, pH optima, metal-ion dependence and susceptibility to inhibitors. Further, this novel activity assumes significance since PTPRδ is predominantly expressed in the brain and is involved in guiding and termination of motor neurons during embryonic development. Since glycosaminoglycans, a family of linear sulfated polysaccharides, play important roles in neuronal growth, regeneration and plasticity (19), their sugar hydrolase activity may not be accidental and may indicate an important physiological role that this phosphatase plays vis-à-vis nerve growth. Finally, this work suggests that unexplored promiscuous activities may constitute an important pool of chemistries, deduction of which would help unravel the complexities of metabolism.

Experimental methods

Reagents

All reagents and chemicals, unless mentioned otherwise, were of high quality and were procured from Sigma-Aldrich Co. (St. Louis, MO), Amresco (Solon, OH) and Fisher Scientific (Hampton, NH). Media components were from Amresco (Solon, OH) Macrosep centrifugal devices were from Pall Co., (Port Washington, NY). The expression clones for the phosphatase domain of PTPRδ (RnCD00383366) and PTPRΩ (HsCD00423639) were procured from DNASU plasmid repository, Arizona State University. The identity of the supplied clones was confirmed by DNA sequencing.

Bioinformatics analysis

The sequence of r-PTPRδ and other PTPRs were obtained from NCBI. The non-redundant database at NCBI was used to search for homologs of PTPRδ using the algorithm BLASTP. Distant homology searches were carried out using PSI-BLAST (20). T-Coffee (21) was used for generating multiple sequence alignment profiles. Phylogenetic and molecular evolutionary analyses were done using MEGA, version 3.1 (22). Molecular visualization and structure analysis were done using various tools like SPDBV (23), PyMOL (pymol.sourceforge.net) and CCP4 suite of programs (24).

Expression and purification

The expression plasmids were transformed into *Escherichia coli* DH5α cloning strain for the purpose of routine plasmid isolation and *E. coli* BL21 (DE3) for expression. The transformed cells were grown in terrific broth with kanamycin (50 μg/ml) as the selection marker and induced with IPTG at a final concentration of 0.3 mM. Induction was carried out at 17 °C for 8 hours. The cells were pelleted down at 2600 x g for 20 minutes and were resuspended in 30 ml of lysis buffer (50 mM Tris HCl, pH 7.4, 100 mM NaCl, 2 mM DTT and 10 % glycerol). The cells were lysed using a sonicator (40 % amplitude, 3 seconds on 5 seconds off for 35–40 cycles) yielding crude extract (CE) that was centrifuged at 12900 x g for 30 min. The supernatant (referred to as the soluble fraction, SE) was kept for binding with equilibrated nickel nitrilotriacetic acid (Ni-NTA) beads (Perfectflow Ni-NTA superflow 5-Prime GmbH, Hilden, Germany) for 3 hrs while the pellet, representing the in-soluble fraction (ISF), and beads (BE) were stored to assess possible loss of protein on SDS-PAGE gel. After 3 hrs, the beads with the protein of interest was pelleted down and the flow-through containing *E. coli* background protein was collected to test on SDS-PAGE gel (FT). The beads were washed extensively with 30 ml of wash buffer (lysis buffer containing 0mM, 15 mM and 20 mM imidazole, respectively)(WI, W-II and W-III fractions in Fig 1A). The bound enzyme was eluted with 5 ml of elution buffer (lysis buffer containing 250 mM imidazole). After the elution of the protein from Ni-NTA beads (E), EDTA was added to a final concentration of 1mM to prevent oxidation by trace nickel contamination. The protein was concentrated to required volume using Macrosep centrifugal devices (Pall Co., USA) with 10 KDa cutoff membrane and stored at −80 °C. SDS-PAGE analysis was performed using standard protocols (25). Protein concentrations were determined by the method of Bradford (26) with bovine serum albumin (BSA) as a protein standard.

Protein purity assessment

The purity of the protein preparation was assessed by overloading the protein on an SDS-PAGE and by performing mass-spectrometric analysis on a Q Exactive™ Plus Mass spectrometer. The latter instrument is designed for accurate quantitation of low-abundance analytes and superior trapping of large molecules for improved analysis of intact proteins.

For intact mass determination of PD-PTPRδ, the protein was processed as follows: The recombinantly expressed and purified protein was extensively dialyzed into 10 mM ammonium acetate using Sartorius Vivacon 500 microfiltration devices (2,000 molecular weight cut-off filters) to remove nonvolatile salts and glycerol. It was then resuspended at a concentration of 300 ng/μL in 50% acetonitrile/49% water/1% acetic acid for direct infusion into a Q Exactive Plus Mass Spectrometer (Thermo Scientific) via the HESI-II source (Thermo Scientific). The instrument was operated in positive ESI mode with a sheath gas flow of 12 units, Auxiliary gas of 3 units and no sheath gas flow, a spray voltage of 5.0 kV, and a capillary temperature of 285 °C. The automatic gain control (AGC) targets of 1×10^6 with a maximum injection time of 200 ms, and five (5) microscans were combined per spectra. Spectra were averaged using Qual Browser Ver. 3.0.63 (Thermo Scientific) and deconvoluted manually. The mass-spectrometric analysis was repeated thrice with three independent batches of protein.

Activity measurements using pNPP as the substrate

To determine the kinetic parameters of the phosphatase activity for PD-PTPRδ and PD-PTPRΩ, the rate of p-nitrophenyl phosphate (pNPP) (Sigma, St. Louis, MO, USA) hydrolysis was determined by monitoring the increase in absorbance at 405 nm for 300 seconds. A molar extinction coefficient (ε) of 18,000 $M^{-1}cm^{-1}$ for p-nitrophenol at 405 nm was used to compute the amount of product formed from the slope of initial velocity curves (27). The non-enzymatic hydrolysis of pNPP was normalized by monitoring the reaction in a double beam Hitachi U-2010 UV-Vis spectrophotometer (Hitachi High Technologies America, Inc., San Jose, CA, USA) with an appropriate blank. Assays were initiated with the addition of enzyme to the sample cuvette after zeroing the absorbance reading with respect to the reference cuvette. The initial velocities were measured for reaction mixtures containing 100 mM HEPES pH 7.3 at room temperature (~ 22 ° C).

To determine the K_m and V_{max} for pNPP, the substrate was titrated and the resultant velocities were plotted against substrate concentration and fit to either equation 1 for one-site binding hyperbola in the absence of any substrate inhibition or equation 2 when substrate inhibition was seen.

$$d[P]/dt=(V_{max} \times [S])/(K_m+[S]) \quad (1)$$

$$d[P]/dt=V_{max}/(1+K_m/[S]+[S]/K_{SI}) \quad (2)$$

where d[P]/dt is the rate of product formation, V_{max} is the maximum velocity, [S] is the substrate concentration, K_m is the Michaelis-Menten constant for pNPP and K_{SI} is the substrate-inhibition constant.

All the measurements were performed in duplicate with two independent experiments done and the resulting error values are reported as their standard deviation (S.D.). To rule out the effect of ionic strength interfering with phosphatase activity due to metal ion addition, Mg^{2+} ion was titrated at saturating pNPP, and it was demonstrated that the activity remains constant. The concentration of PD-PTPRδ and PD-PTPRΩ used was 58 nM for pNPP hydrolysis. Unless mentioned otherwise, all the data were fit using linear regression and non-linear curve fitting subroutines of GraphPad Prism, version 4.0 (GraphPad Software, Inc., San Diego, CA).

Phosphate estimation by Chen's assay

The assays were carried out under initial velocity conditions where the product formed was less than 5% of the initial substrate concentration. 100 μl of reaction volume contained 100 mM HEPES, pH 7.3, 15 mM $MgCl_2$, and varying concentrations of substrate. Various substrates including o-phosphotyrosine, adenosine monophosphate, inosine monophosphate, guanosine monophosphate, nicotinamide adenine dinucleotide phosphate and pyridoxal 5′-phosphate were tested (Table 1). The enzyme showed hydrolysis of o-phosphotyrosine

alone. The reaction was initiated by addition of 58 nM enzyme and allowed to proceed for 5 min. for phosphotyrosine at 37 °C. The reaction was quenched by addition of 20 μl of 70 % TCA. The reaction mixture was centrifuged at 9500 x g for 10 min., and the supernatant was added to 1 ml of Chen's reagent (6 N sulfuric acid, distilled water, 2.5 % ammonium molybdate and 10 % ascorbic acid mixed in 1:2:1:1 ratio). The reaction mix was allowed to incubate at 37 °C for 30 min. for color stabilization. The absorbance was recorded at 820 nm (molar extinction coefficient is 25000 M^{-1} cm^{-1}) with a double beam Hitachi U-2010 UV-Vis spectrophotometer (Hitachi High Technologies America, Inc., San Jose, CA, USA).

To determine the K_m and V_{max} for phosphotyrosine, the substrate was titrated and the resultant velocities plotted against substrate concentration. The data were fit to Hill equation (3)

$$d[P]/dt=(V_{max} X [S]^h)/([K]_{0.5}{}^h+[S]^h) \quad (3)$$

where d[P]/dt is the velocity, V_{max} is the maximum velocity, [S] is the substrate concentration, $[K]_{0.5}$ is the substrate concentration at half maximal velocity and h is the Hill's coefficient.

Pre-steady state kinetics

The pre-steady state kinetics for pNPP hydrolysis of PD-PTPRΩ was monitored in a double beam Hitachi U-2010 UV-Vis spectrophotometer with an appropriate blank given that the burst phase lasted for ~50 sec. Absorbance at t=0 was subtracted from the rest of the data and absorbance plotted against time. Two measurements were averaged, and the data were fit to equation (4)

$$A_{405}=v_s t+((v_0-v_s)/k)\,(1-\exp\hat{}(-kt))+c \quad (4)$$

where t is time in seconds, v_0 is initial velocity, v_s is steady state velocity, k is the apparent pseudo-first order rate constant for the transition from v_0 to v_s and c is the initial absorbance at 405 nm. Enzyme titration was carried out to ascertain whether the magnitude of burst increases with increasing enzyme concentration at 9.6 nM–96.1 nM.

Inhibition kinetics

The inhibitory effect of phosphate and orthovanadate on the phosphomonoester hydrolysis activity of PD-PTPRδ and PD-PTPRΩ were assessed experimentally. Both the potency of the inhibitor and its affinity for the enzyme were computed by experimental IC-50 determinations. IC-50 determination assays were carried out in 100 mM HEPES pH 7.3, 5 mM pNPP and variable concentration of each inhibitor. The enzyme concentration was as specified above. Inhibitory potential of the covalent inhibitor NEM was also assessed on the phosphomonoester hydrolysis activity of PTPRΩ. The curves were fit to equation (5), where I is the inhibitor concentration, and y is the percentage of activity.

$$y=100\%[1+(I/IC-50)] \quad (5)$$

Furthermore, K_{iapp} were computed from the IC-50 curves by fitting them to the quadratic Morrison equation (6) for tight binding inhibition. This equation accounts for tight binding by doing away with the assumption that the free concentration of inhibitor equals the total concentration.

$$v_i/v_0=1-(([E]_T+[I]_T+K_i^{app})-\sqrt{([E]_T+[I]_T+K_i^{app})^2-4[E]_T\,[I]_T}/2[E]_T \quad (6)$$

where v_i represents velocity in the presence of inhibitor, v_0 represents velocity in the absence of inhibitor, $[E]_T$ represents total enzyme, $[I]_T$ represents total inhibitor and K_i^{app} represents apparent K_i.

pH kinetics

The pH dependence of PTPRδ's phosphatase activity (k_{cat} and k_{cat}/K_m) and sugar hydrolase activity was monitored over the pH range 6.0–9.0. Pre-incubation of the enzyme in different pH buffers (5.5–8.5) did not cause any irreversible loss in activity. However, there was a minor loss of activity below pH 5.5 and hence the analysis was carried out only till pH 5.5. Thus, the inflections observed in the pH profile from 5.5–8.5 can be approximated to the true ionizations of the enzyme's catalytic groups. k_{cat} is the 1st order rate constant. Its variation with pH is reflective of the ionization events in the catalytic complex. On the other hand, k_{cat}/K_m is the 2nd order rate constant indicative of ionization(s) of either the free substrate or the free enzyme towards the catalytic complex formation. The kinetic parameters, k_{cat} and k_{cat}/K_m obtained from each plot at different pH values were plotted as a function of pH to Eqs. (7) and (8) describing double and single ionization(s), respectively.

$$y=c/\{1+([H]/K_1)+(K_2/[H])\} \quad (7)$$

$$y=c/\{1+K_2/[H])\} \quad (8)$$

where y is the pH dependent parameter, c is the pH independent value of the parameter, [H] is the hydrogen ion concentration and K_1 and K_2 are the ionization constants for the ionizable groups involved in catalysis. pH of the assay mixture was adjusted with 50 mM mixed buffer (MES, PIPES and HEPES) and temperature kept constant at 25 °C.

Sugar hydrolysis assay

O-nitrophenyl β-galactopyranoside (ONPG), an analog of lactose, is an artificial substrate used to assay the β-galactosidase activity of an enzyme. Since the reactions rates were slow,

all the assays were carried out as endpoint measurements. Assays were initiated with the addition of enzyme to the test reactions. A blank reaction without the enzyme was maintained to normalize for non-catalytic hydrolysis of substrate. The quantity of the enzyme used varied depending on the length of incubation and the type of assay carried out. However, the enzyme concentration was kept constant between the test and the control for a given assay for ease of comparison. The reaction was terminated with the addition of 200 μl of Na_2CO_3. Liberated O-nitrophenol was measured at 420 nm. The amount of product formed was computed from the absorbance reading using an ε value of 4.5 X 10^3 $M^{-1}cm^{-1}$(28). Further, other artificial substrates p-nitrophenyl β-galactoside (PNPG), p-nitrophenyl β-glucuronide (PNPGlucu), p-nitrophenyl α-D-glucoside (4NGU-alpha) and p-nitrophenyl α-D-galactoside (4NGA-alpha) and p-nitrophenyl N-actyl-β-D glucosaminide (4NP-NA-GU) were also assessed for their hydrolysis by the phosphatase domain of PTPRδ and PD-PTPRΩ (Table 1).

Binding assays

Differential scanning fluorimetry was carried out as described in previous studies (29–32). Briefly, 10 μM protein was used and the extrinsic fluorophore dye Sypro-orange was employed to detect unfolding in the presence and absence of 100 μM, 500 μM and 1000 μM small-molecule ligands.

Results

Novel sugar hydrolase activity on the phosphatase domain of PTPRδ

It has been recently demonstrated that the library of native pockets is covered by a remarkably small number (~400) of representative pockets (9). With that in mind, one might expect that basal enzymatic activity is an inherent feature of those pockets having an accidental juxtaposition of residues that have been demonstrated to have a role in catalysis (33, 34). Indeed, native like enzymatic pockets with catalytic residue types and geometries are reproduced in proteins lacking any selection for enzymatic function (9, 10). With these results in mind, we selected the phosphatase domain of PTPRδ as the protein of interest. The protein was expressed and purified to homogeneity (Fig 1A). Systematic screens for hydrolase function, with phosphoester, glycosidic and peptide bond hydrolysis as representative activities were set up (Table 1). As the name implies, the phosphatase domain of PTPRδ functions as a hydrolase that catalyzes phosphomonoester hydrolysis of phosphorylated tyrosine residues on proteins. As expected, the protein showed good phosphatase activity as is evident in the hydrolysis of the artificial substrate p-nitrophenyl phosphatase, an analogue of phosphotyrosine (Fig 1B) (Table 2). Surprisingly, the protein also showed activity with the o-nitrophenyl galactoside (ONPG) substrate. However, the activity was much feebler than for the phosphomonoester bond hydrolysis (Fig 1C and 1D). ONPG is a mimic of lactose and is a substrate that is routinely employed for assaying β-galactosidase activity. To ensure that the observed activity is not an artifact, a close homologue of the protein, the phosphatase domain, PD, of PTPRΩ, was expressed, purified to homogeneity and assayed for possible sugar hydrolase activity. PD-PTPRΩ shares 43.34 % sequence identity to PD-PTPRδ (Fig S1A) and has the same overall global fold (Fig S1B). As expected, PD-PTPRΩ also showed hydrolysis of ONPG (Fig 1D). However,

PD-PTPRδ hydrolyzes the sugar substrates ~1.5–2 fold better than PD-PTPRΩ. The enzyme concentration dependence of sugar hydrolase activity for PD-PTPRδ showed a linear increase providing additional proof that the origin of the activity is in the purified recombinant protein (Fig S1C). Since, among the three distinct substrate classes tested (Table 1), the enzyme hydrolyzed both the phosphomonoester and the sugar substrates, it could be speculated that it is a non-specific hydrolase. However, both PD-PTPRδ and PD-PTPRΩ failed to show any discernible peptide hydrolysis activity even after incubating the substrate with repeated supplementation of high concentrations of enzyme every 12 hrs. (Fig S1D). All these experiments indicate that the sugar hydrolase activity indeed originates from the phosphatase domain of PTPRδ and is highly specific for the hydrolysis of both glycosidic and phosphomonoester bonds.

It is understood that the purity of the protein preparation is a major criterion in such kind of studies as use of impure enzyme can lead to aberrant results. The mass and purity of the protein were assessed by overloading the protein on an SDS-PAGE gel and by carrying out mass spectrometric analysis (Fig 2). Mass spectrometric analysis can not only yield the protein's identity through comparison with the expected mass of the protein of interest, but also the relative purity of the sample based on the ratio of the desired mass peak to other mass peaks in the sample (35, 36). The intact mass was determined to be 34167 Da based on direct infusion into a high mass accuracy mass Q Exactive Plus mass spectrometer. This is in close agreement with the theoretical average mass of 34167.5 corresponding to the protein sequence with its N-terminal methionine cleaved. Further, the presence of the stereotypical isotope clusters of the various charge states with no other overlapping clusters suggests that no other contaminating proteins are present (Fig 2). The SDS-PAGE gel overloaded with 30 μg and 50 μg PD-PTPRδ also does not show any visible contaminants (Fig 2 inset). Further, it has to be noted that the activity was consistent across different batches of proteins purified and across two different proteins viz., PD-PTPRδ and PD-PTPRΩ tested.

The literature is replete with examples of catalytic promiscuity with the most prominent example being that of proteases (catalyzing the hydrolysis of C-N bond) also carrying out ester (C-O) hydrolysis (37). However, to the best of our knowledge, our example is the first instance of a single enzyme catalyzing the hydrolysis of a COP bond and a COC bond.

Characterization of monoesterase activity of PD-PTPRδ and PD-PTPRΩ

Though the phosphatase domains of other PTPRs have been characterized, there are no studies that report the kinetic characterization of either PD-PTPRδ or PD-PTPRΩ. Detailed kinetic analysis was carried out to assess the hydrolysis of phosphorylated substrate by PD-PTPRδ and PD-PTPRΩ. Hydrolysis of the artificial substrate p-nitrophenyl phosphate (pNPP) was monitored both in a continuous assay by monitoring p-nitrophenyl liberation and in an end point assay by monitoring for the liberated phosphate through Chen's assay (38). As expected, the enzymes showed activity against pNPP with a rate enhancement of ~ 10^{17} compared to the uncatalyzed reaction (Table 2). This rate enhancement corresponds to that displayed by other phosphatases (39). PD-PTPRΩ showed better pNPP hydrolyzing activity than PD-PTPRδ; though the time-dependence of substrate to product conversion by PD-PTPRδ was linear, PD-PTPRΩ showed a biphasic plot indicative of a burst followed by

a steady state (Fig 3A). Pre-steady state kinetic analysis showed that the magnitude of the burst phase was dependent on protein concentration (Fig 3B–C) and vanished with increasing N-ethylmaleimide (NEM) (Fig 3D). NEM is an irreversible inhibitor of enzymes with active site cysteine residues and is widely employed to probe the role of thiol groups in enzyme mechanism studies. Inhibition and the vanishing burst phase in the presence of NEM is indicative of the phosphocysteinyl intermediate hydrolysis being the rate-limiting step in PD-PTPRΩ (Fig 3E). Receptor protein tyrosine phosphatases (PTPRs) are known to employ a cysteine nucleophile to attack the incoming phosphorylated substrate to form the phosphoenzyme intermediate on the reaction coordinate. Sequence analysis and structural superposition of the various PTPRs showed that the motif HCXXGXGR, pivotal to catalysis and conserved across all the PTPs, is highly conserved in PD-PTPRΩ (Fig S1A). It should be pointed out here that phosphate, which is a reversible inhibitor of the enzyme activity, doesn't abolish the burst phase (Fig 3F). The pNPP hydrolyzing activity of the PTPRΩ and PTPRδ enzymes was inhibited by phosphate with mM IC-50 values indicative of poor affinity for the active site (Fig S2A). On the contrary, orthovanadate potently inhibited the pNPP hydrolyzing activity of PTPRδ with a K_i^{app} of 120.1 ± 12.9 nM (Fig S2B). Phosphotyrosine, when tested as substrate for PD-PTPRδ, did get hydrolyzed but with very poor affinities (Fig S2C and Table 2). Anchoring of the phosphotyrosine moiety on a peptide substrate of interest might be essential for efficient hydrolysis of the substrate. The tyrosine residue failed to inhibit the pNPP hydrolyzing activity of either enzyme indicating that the absence of a phosphate moiety yields a metabolite with no affinity whatsoever for the active site of the two enzymes.

To further understand the specificity of the PTP active site, a range of phosphate monoesters were assessed to monitor their hydrolysis (Table 1). The substrates tested included different nucleoside monophosphates and pyridoxal phosphate. The enzymes didn't show any detectable activity against the above substrates indicating that the active site is highly specific for the hydrolysis of their intended substrate.

The affinity and turnover of the substrate pNPP for PD-PTPRδ was assayed at several different pH values to understand the pH optima for the hydrolysis of the phosphorylated substrate. The plot of k_{cat} versus pH was a bell shaped curve with both acidic and alkaline limbs (Fig 4A). The pH dependence of k_{cat} of PD-PTPRδ towards the substrate pNPP indicated that one group must be unprotonated (pKa ~4.72) and one group must be protonated (pKa ~7.4) for effective catalysis. Similarly, the plot of k_{cat}/K_m also showed a reasonable fit to the equation for two ionizations, but did not converge to a good fit when the equation for single or triple ionization was employed (Fig 4B). However, the alkaline limb was more pronounced with a pKa of ~6.65. The acidic limb lacked points due to possible enzyme denaturation below pH 5.5 (see Materials and Methods). However, an approximation of the pK_a for the acidic limb gave an estimate of 4.72, similar to that obtained from the k_{cat} versus pH plot. This, once again, indicates that one group is likely unprotonated (pKa ~4.72) and one group protonated (pKa ~6.65) on either the substrate or the enzyme to enable effective catalytic complex formation. However, it should be noted here that the pKa values presented for the acidic limb are mere extrapolations from the fits and should be considered as approximate estimates of the values.

In spite of the pH optima for activity being around pH 6.3, all phosphatase activity assays were performed at pH 7.3 in order to reduce the non-catalytic hydrolysis of the substrate. Table 2 summarizes the kinetic parameters, and Fig 4C and Fig S2D shows the substrate vs velocity plot of both PD-PTPRδ and PD-PTPRΩ for the phosphorylated substrate pNPP, respectively. The values of K_m and k_{cat} for PD-PTPRΩ were obtained from slopes taken both from the burst phase and the steady state phase (Fig S2D). As seen in the figure, PD-PTPRΩ shows substrate inhibition with pNPP that is absent in the substrate vs velocity plot for PD-PTPRδ. This differential behavior can be exploited in the discovery of homologue specific inhibitors against the two enzymes.

Characterization of diesterase activity of PD-PTPRδ and PD-PTPRΩ

Monoesterases are highly specific for monoester hydrolysis and do not usually display diesterase activity. As an exception, alkaline phosphatase is known to display both monoesterase and diesterase activity (40). However, the latter activity is far weaker than the principal activity of monoester hydrolysis. It came as a surprise when the phosphatase domain of PTPRδ displayed diesterase activity on the artificial substrate bis-pNPP in spite of the highly discriminative nature of the active site towards a particular kind of phosphate monoester (Table 1). It should be pointed out that the diesterase activity was also detected with the close homologue PTPRΩ (Fig S2E). Fig 4D shows the substrate vs velocity plot for bis-pNPP hydrolysis for PD-PTPRδ. However, the curve failed to saturate even at a high concentration of 60 mM making it difficult to estimate reliable kinetic parameters. The diesterase activity was also inhibited by NEM, once again implicating an active site cysteine in catalyzing both monoesterase and diesterase activities from the same active site pocket (Fig S4A). Moreover, this suggests that the enzyme displays substrate promiscuity. Designing of specific inhibitors for phosphatases has confounded medicinal chemists because of the high-conservation of the P-loop. Our findings, that the enzymes act on diesterases in addition to their primary role as monoester hydrolases and show different behavior in hydrolyzing their monoester substrates, assumes significance from the perspective of designing specific inhibitors for this class of enzymes.

A range of analogues of pNPP and bis-pNPP were assessed to see whether the enzyme could act on them given the promiscuity it displays towards monoester and diester hydrolysis. Fig S3 shows the structures of the various analogues employed. It is interesting to note that the enzyme hydrolyzed none of them. Further, they neither show inhibition of the phosphatase activity for pNPP hydrolysis nor did they bind to the enzyme as assessed by differential scanning fluorimetry. This indicates that the enzyme is intolerant to any substitutions on the phosphate group of either pNPP or bis-pNPP, and hence, binding of and activity on these substrates are mainly dependent on the presence of the phosphate group. This observation makes the activity shown on sugar substrates ONPG and PNPG by the enzymes all the more significant.

Characterization of sugar hydrolase activity of PD-PTPRδ and PD-PTPRΩ

Having confirmed the sugar hydrolysis activity as emerging from PD-PTPRδ and PD-PTPRΩ, we tested a range of sugars as possible substrates of the enzyme (Table 1). Before undertaking further kinetic characterization, the metal ion dependence of the sugar hydrolase

activity was assessed (Table S1 and Fig 5A). The sugar hydrolysis activity increases ~1.5 fold in the presence of the divalent cation magnesium and monovalent cation potassium (Fig 5A). This dependence of the sugar hydrolysis activity on both the divalent and monovalent cation is highly similar to that shown by conventional sugar hydrolases (41). It should be pointed out here that the phosphatase activity of the enzyme is independent of either divalent or monovalent metal ions (Fig S2F). However, phosphatases from the HAD superfamily are metal-dependent enzymes relying on the presence of divalent cations for catalysis of the phosphomonoester bond (42). Assaying the various sugars indicated that PNPG was the best substrate followed by the other sugars (Fig 5B). The pH dependence of the sugar hydrolysis activity indicated a pH optimum of ~7.3 (Fig 5C), which is markedly different from that displayed for the phosphatase activity (pH 6.3). Detailed kinetic characterization of the sugar hydrolase activity was not possible since the activity against sugar substrates was extremely slow and couldn't be carried out without resorting to a non-catalytic amount of the enzyme. However, we were able to assess the apparent affinity (K_m^{app}) and apparent maximum velocity (V_{max}^{app}) of the enzyme for the substrate ONPG by incubating the reaction with 1 μM enzyme at 37°C for ~19 hours. The enzyme, under the conditions of the assay, showed conventional Michaelis-Menten hyperbolic behavior in hydrolyzing ONPG (Fig 5D). The sugar hydrolyzing activity was markedly inhibited in the presence of IPTG and mildly inhibited with lactose, both structural analogues of the sugar substrates employed (Fig 5E–F). It should be pointed out that the assay was blind to the hydrolysis of lactose, if any, and only reported on the interference of ONPG hydrolysis activity by lactose. Further, it should be noted that IPTG didn't interfere with the phosphomonoester hydrolysis activity of PD-PTPRδ (Fig S4B). On the contrary, phosphate didn't interfere with the sugar hydrolase activity even at 30 mM (Fig S4C). However, NEM did show reduction in the sugar hydrolase activity (Fig S4D). This inhibition couldn't be further assessed because of the extremely slow reaction rates and maybe indicative of the involvement of cysteine either in catalysis or the binding of ONPG to enzyme.

Discussion

Latent promiscuous enzyme activities might constitute an important pool of chemistries that might confound our understanding/modeling of metabolism. For instance, 37% of the enzymes in *Escherichia coli* genome show promiscuous activities and 65 % of the known metabolic reactions arise from such generalist enzymes (43). The latter number represents a huge fraction of the total chemistries that take place in a cell, and unlike the way traditional enzymology is done, the emphasis of future enzymatic studies should be on the unraveling and characterization of such latent activities.

It has been shown in the past that substrate promiscuity is a far more frequent occurrence in a genome than catalytic promiscuity. Moreover, it has been argued that even in cases where catalytic promiscuity is seen there needs to be a common substrate substructure that might facilitate the binding and hence, catalysis i.e., an appropriate anchor group or chemophore might lead the substrate to bind to a larger, and often diverse, number of pockets with the right alignment of active site residues (44). In fact, in a previous study from our group, we have demonstrated that the limited number of geometrical pockets that are present in biologically occurring proteins (9) suggests that promiscuity should be the rule rather than

exception. Given the small fraction of amino acids that are usually found in the active sites of enzymes and the high probability of their co-occurrence in other pockets (9, 10, 33, 34), lead us to conclude that promiscuous activities ought to be more widespread than was previously assumed.

As an important case study with possible implications to the physiological functionality of the protein, we have demonstrated a novel sugar hydrolase activity for PD-PTPRδ and PD-PTPRΩ. The finding assumes significance because of the crucial role these phosphatases play in the signal transduction pathways of neuronal growth. Further, demonstration of catalytic promiscuity (as in the hydrolysis of COC bond apart from the usual COP bond) and substrate promiscuity (hydrolysis of substrates with diester bonds as well as monoester bonds) yet retaining substrate discrimination is indicative of the fine balance that determines promiscuity vs specificity even when catalyzing diverse reactions. It can be speculated that the common nitrophenyl anchor group might have contributed to the recognition across the three substrate types. However, as demonstrated with substrate analogues for pNPP and bis-pNPP that do not act as either substrates or inhibitors (Fig S3), it is highly unlikely that the nitrophenol moiety might be the determinant for either binding or catalysis. This assumption is further confirmed due to the lack of inhibition of pNPP hydrolysis activity shown by the tyrosine residue. Marked differences in the rates and conditions of catalysis render these reactions unique and specific (Fig 6). For instance, though the phosphatase reaction is inhibited by phosphate and orthovanadate, they do not have any effect on the sugar hydrolysis activity of the enzyme. Further, IPTG affects sugar hydrolysis activity with no interference whatsoever in the phosphatase reaction. The differential metal ion dependence for the two activities constitutes another important difference that indicates differential mechanistic details for the two reactions. These differences lead us to speculate that the activities might be emerging from two distinct pockets on the protein. We call such enzymes dizymes and posit that they will be important in regulation of cellular metabolism. If the product of one active site modulates the enzymatic behavior of the other site, then having both chemistries in the same domain may exert local biochemical control in a cellular context.

To the best of our knowledge, this is the first study that shows both substrate promiscuity and catalytic promiscuity in an enzyme domain. Yet, the enzyme demonstrates discrimination and specificity in catalyzing the hydrolysis of monoester and diester substrates. These promiscuous functionalities assume more significance in the light of PTPRδ's important role in neuronal development and its significant sequence identity with PTPRσ (a closely related phosphatase with ~ 85% sequence identity) and Leucocyte common antigen related protein (LAR) that have been implicated in several malignancies and life-style disorders (45–47). It has to be noted here that a lot of their role in neuronal processes stems from the ability of their extracellular domains to interact with proteoglycans, which are degraded intracellularly, and the promiscuous activity displayed by the intracellular phosphatase domain may not be of mere interest in understanding the underlying mechanistic details but may have real physiological roles (48–51).

The order of magnitude differences in the rates of hydrolysis across the monoesterase, diesterase and glycosidic bond hydrolysis activities may indicate that the poor activities

might possibly represent evolutionary repositories for future enzymatic functions. However, it has not escaped our notice that the physiologically relevant substrates may not have been assayed and in spite of our broad screen across three different substrate classes and two enzymes, we may have missed the preferred sugar and diesterase substrates that the enzyme acts upon in the cellular milieu. However, it would be a difficult task to assay all possible substrates that possess a COC bond or a diester bond given the myriad number of leaving groups that might require different assay systems for detection. For instance, the presence of COC bonds across various sugars and O-linked glycoproteins makes it a daunting task to devise specific assays for a single study. However, we believe that our study and its findings would pave the way for future enquiries into possible substrate preferences for these enzymes.

Design of specific inhibitors for phosphatases has been another challenging research area. The high conservation of the active site across the various phosphatases often leads to extensive non-specificity for the designed inhibitor rendering it clinically irrelevant (52). Another important insight that emerges from our study is the differences between PD-PTPRδ and PD-PTPRΩ that could be potentially exploited in designing specific inhibitors for the respective phosphatase. PD-PTPRΩ shows rate-limiting phosphocysteinyl hydrolysis leading to a biphasic time-dependence of substrate to product conversion. The absence of this detectable rate-limiting step in PD-PTPRδ combined with the significant difference in the velocity of hydrolysis for pNPP and the sugar substrate for the two proteins indicate avenues that could be further utilized for discovery of specific inhibitors. Another difference is the substrate inhibition seen with PD-PTPRΩ that is absent in PD-PTPRδ. Substrate inhibition like behavior usually arises because of an alternate site of binding and is possibly indicative of a novel pocket distinct from the active site that could be targeted for drug-discovery purposes.

In summary, this study is the first to report the multiple distinct chemistries that are catalyzed by the phosphatase domain of PD-PTPRδ and PD-PTPRΩ. The chemistries fall into the domain of both substrate promiscuity and catalytic promiscuity. Further, we also demonstrate convincing differences between the two closely related phosphatases that can be exploited to design specific inhibitors for the respective phosphatases. In conclusion, we posit that occurrence of promiscuous activities on enzymes is the rule rather than the exception and systematic screens to unravel such interactions would facilitate a better understanding of metabolism. This conclusion stems from the important insights provided by previous studies from our group linking the physics of protein folding and the presence of background biochemical activities (9, 10, 53, 54). In those studies, comparison of artificially generated compact protein structures (ART protein library) selected for thermodynamic stability but not for function, demonstrates that a remarkable number of properties of the native-like proteins are recapitulated. These include the complete set of small molecule ligand-binding pockets and most protein-protein interfaces. ART structures are predicted to weakly bind metabolites that are components of a significant fraction of metabolic pathways, with the most enriched pathway being glycolysis. Native-like active sites are also found in ART proteins. Overall, it appears that biochemical function is an intrinsic feature of proteins which nature has significantly optimized during evolution. As an extension of this hypothesis, the current study presents the first experimental evidence for the presence of

such random background activity by the demonstration of a sugar hydrolase activity on the phosphatase domain of PD-PTPRδ and PD-PTPRΩ.

Supplementary Material

Refer to Web version on PubMed Central for supplementary material.

Acknowledgments

The authors wish to thank DNASU for providing the expression plasmids for clones of PD-PTPRδ and PD-PTPRΩ. We would also like to thank the Developmental Therapeutics Program of the National Cancer Institute for providing the small molecules used in this study.

Funding information:

This project was funded by GM-48835 of the Division of General Medical Sciences of the NIH.

Abbreviations

PTPRδ	Protein Tyrosine Phosphatase delta
PTPRΩ	Protein Tyrosine Phosphatase omega
PD-PTPRδ	Phosphatase domain of PTPRδ
PD-PTPRΩ	Phosphatase domain of PTPRΩ

References

1. Pandya C, Farelli JD, Dunaway-Mariano D, Allen KN. Enzyme promiscuity: engine of evolutionary innovation. The Journal of biological chemistry. 2014; 289(44):30229–36. [PubMed: 25210039]
2. Babtie A, Tokuriki N, Hollfelder F. What makes an enzyme promiscuous? Current opinion in chemical biology. 2010; 14(2):200–7. [PubMed: 20080434]
3. Khersonsky O, Roodveldt C, Tawfik DS. Enzyme promiscuity: evolutionary and mechanistic aspects. Current opinion in chemical biology. 2006; 10(5):498–508. [PubMed: 16939713]
4. O'Brien PJ, Herschlag D. Catalytic promiscuity and the evolution of new enzymatic activities. Chemistry & biology. 1999; 6(4):R91–R105. [PubMed: 10099128]
5. Jensen RA. Enzyme recruitment in evolution of new function. Annual review of microbiology. 1976; 30:409–25.
6. Srinivasan B, Kempaiah Nagappa L, Shukla A, Balaram H. Prediction of substrate specificity and preliminary kinetic characterization of the hypothetical protein PVX_123945 from Plasmodium vivax. Experimental parasitology. 2015; 151–152:56–63.
7. Glasner ME, Gerlt JA, Babbitt PC. Evolution of enzyme superfamilies. Current opinion in chemical biology. 2006; 10(5):492–7. [PubMed: 16935022]
8. Kazlauskas RJ. Enhancing catalytic promiscuity for biocatalysis. Current opinion in chemical biology. 2005; 9(2):195–201. [PubMed: 15811805]
9. Skolnick J, Gao M, Zhou H. On the role of physics and evolution in dictating protein structure and function. Israel journal of chemistry. 2014; 54(8–9):1176–88. [PubMed: 25484448]
10. Skolnick J, Gao M, Zhou H. How special is the biochemical function of native proteins? F1000Research. 2016:5.
11. Rye CS, Withers SG. Glycosidase mechanisms. Current opinion in chemical biology. 2000; 4(5): 573–80. [PubMed: 11006547]
12. Zechel DL, Withers SG. Glycosidase mechanisms: anatomy of a finely tuned catalyst. Accounts of chemical research. 2000; 33(1):11–8. [PubMed: 10639071]

13. Tiganis T, Bennett AM. Protein tyrosine phosphatase function: the substrate perspective. The Biochemical journal. 2007; 402(1):1–15. [PubMed: 17238862]
14. Ensslen-Craig SE, Brady-Kalnay SM. Receptor protein tyrosine phosphatases regulate neural development and axon guidance. Developmental biology. 2004; 275(1):12–22. [PubMed: 15464569]
15. Stepanek L, Stoker AW, Stoeckli E, Bixby JL. Receptor tyrosine phosphatases guide vertebrate motor axons during development. The Journal of neuroscience: the official journal of the Society for Neuroscience. 2005; 25(15):3813–23. [PubMed: 15829633]
16. Gonzalez-Brito MR, Bixby JL. Differential activities in adhesion and neurite growth of fibronectin type III repeats in the PTP-delta extracellular domain. International journal of developmental neuroscience: the official journal of the International Society for Developmental Neuroscience. 2006; 24(7):425–9. [PubMed: 17034983]
17. Uetani N, Kato K, Ogura H, Mizuno K, Kawano K, Mikoshiba K, et al. Impaired learning with enhanced hippocampal long-term potentiation in PTPdelta-deficient mice. The EMBO journal. 2000; 19(12):2775–85. [PubMed: 10856223]
18. Shen Y, Tenney AP, Busch SA, Horn KP, Cuascut FX, Liu K, et al. PTPsigma is a receptor for chondroitin sulfate proteoglycan, an inhibitor of neural regeneration. Science. 2009; 326(5952): 592–6. [PubMed: 19833921]
19. Swarup VP, Mencio CP, Hlady V, Kuberan B. Sugar glues for broken neurons. Biomolecular concepts. 2013; 4(3):233–57. [PubMed: 25285176]
20. Altschul SF, Madden TL, Schaffer AA, Zhang J, Zhang Z, Miller W, et al. Gapped BLAST and PSI-BLAST: a new generation of protein database search programs. Nucleic acids research. 1997; 25(17):3389–402. [PubMed: 9254694]
21. Notredame C, Higgins DG, Heringa J. T-Coffee: A novel method for fast and accurate multiple sequence alignment. Journal of molecular biology. 2000; 302(1):205–17. [PubMed: 10964570]
22. Kumar S, Tamura K, Nei M. MEGA3: Integrated software for Molecular Evolutionary Genetics Analysis and sequence alignment. Briefings in bioinformatics. 2004; 5(2):150–63. [PubMed: 15260895]
23. Guex N, Peitsch MC. SWISS-MODEL and the Swiss-PdbViewer: an environment for comparative protein modeling. Electrophoresis. 1997; 18(15):2714–23. [PubMed: 9504803]
24. Collaborative Computational Project N. The CCP4 suite: programs for protein crystallography. Acta crystallographica Section D, Biological crystallography. 1994; 50(Pt 5):760–3. [PubMed: 15299374]
25. Laemmli UK. Cleavage of structural proteins during the assembly of the head of bacteriophage T4. Nature. 1970; 227(5259):680–5. [PubMed: 5432063]
26. Bradford MM. A rapid and sensitive method for the quantitation of microgram quantities of protein utilizing the principle of protein-dye binding. Analytical biochemistry. 1976; 72:248–54. [PubMed: 942051]
27. Gottlin EB, Xu X, Epstein DM, Burke SP, Eckstein JW, Ballou DP, et al. Kinetic analysis of the catalytic domain of human cdc25B. The Journal of biological chemistry. 1996; 271(44):27445–9. [PubMed: 8910325]
28. Becerra M, Cerdan E, Gonzalez Siso MI. Dealing with different methods for Kluyveromyces lactis beta-galactosidase purification. Biological procedures online. 1998; 1:48–58. [PubMed: 12734592]
29. Roy A, Srinivasan B, Skolnick J. PoLi: A Virtual Screening Pipeline Based on Template Pocket and Ligand Similarity. Journal of chemical information and modeling. 2015; 55(8):1757–70. [PubMed: 26225536]
30. Srinivasan B, Skolnick J. Insights into the slow-onset tight-binding inhibition of Escherichia coli dihydrofolate reductase: detailed mechanistic characterization of pyrrolo [3,2-f] quinazoline-1,3-diamine and its derivatives as novel tight-binding inhibitors. The FEBS journal. 2015; 282(10): 1922–38. [PubMed: 25703118]
31. Srinivasan B, Tonddast-Navaei S, Skolnick J. Ligand binding studies, preliminary structure-activity relationship and detailed mechanistic characterization of 1-phenyl-6,6-dimethyl-1,3,5-triazine-2,4-diamine derivatives as inhibitors of Escherichia coli dihydrofolate reductase. European journal of medicinal chemistry. 2015; 103:600–14. [PubMed: 26414808]

32. Srinivasan B, Zhou H, Kubanek J, Skolnick J. Experimental validation of FINDSITE(comb) virtual ligand screening results for eight proteins yields novel nanomolar and micromolar binders. Journal of cheminformatics. 2014; 6:16. [PubMed: 24936211]
33. Bartlett GJ, Porter CT, Borkakoti N, Thornton JM. Analysis of catalytic residues in enzyme active sites. Journal of molecular biology. 2002; 324(1):105–21. [PubMed: 12421562]
34. Holliday GL, Almonacid DE, Mitchell JB, Thornton JM. The chemistry of protein catalysis. Journal of molecular biology. 2007; 372(5):1261–77. [PubMed: 17727879]
35. Acker MGAD. Considerations for the design and reporting of enzyme assays in high-throughput screening applications. Perspectives in Science. 2014; 1:56–73.
36. Scott, JE.; Williams, KP. Validating Identity, Mass Purity and Enzymatic Purity of Enzyme Preparations. In: Sittampalam, GS.; Coussens, NP.; Nelson, H.; Arkin, M.; Auld, D.; Austin, C., et al., editors. Assay Guidance Manual. Bethesda (MD): 2004.
37. Bornscheuer UT, Kazlauskas RJ. Catalytic promiscuity in biocatalysis: using old enzymes to form new bonds and follow new pathways. Angewandte Chemie. 2004; 43(45):6032–40. [PubMed: 15523680]
38. Chen PS Jr, TT, Huber W. Microdetermination of phosphorous. Anal Chem. 1956; 28:1756–8.
39. Zalatan JG, Herschlag D. Alkaline phosphatase mono- and diesterase reactions: comparative transition state analysis. Journal of the American Chemical Society. 2006; 128(4):1293–303. [PubMed: 16433548]
40. O'Brien PJ, Herschlag D. Functional interrelationships in the alkaline phosphatase superfamily: phosphodiesterase activity of Escherichia coli alkaline phosphatase. Biochemistry. 2001; 40(19): 5691–9. [PubMed: 11341834]
41. Juers DH, Matthews BW, Huber RE. LacZ beta-galactosidase: structure and function of an enzyme of historical and molecular biological importance. Protein science: a publication of the Protein Society. 2012; 21(12):1792–807. [PubMed: 23011886]
42. Srinivasan B, Forouhar F, Shukla A, Sampangi C, Kulkarni S, Abashidze M, et al. Allosteric regulation and substrate activation in cytosolic nucleotidase II from Legionella pneumophila. The FEBS journal. 2014; 281(6):1613–28. [PubMed: 24456211]
43. Nam H, Lewis NE, Lerman JA, Lee DH, Chang RL, Kim D, et al. Network context and selection in the evolution to enzyme specificity. Science. 2012; 337(6098):1101–4. [PubMed: 22936779]
44. Khersonsky O, Malitsky S, Rogachev I, Tawfik DS. Role of chemistry versus substrate binding in recruiting promiscuous enzyme functions. Biochemistry. 2011; 50(13):2683–90. [PubMed: 21332126]
45. Jacob ST, Motiwala T. Epigenetic regulation of protein tyrosine phosphatases: potential molecular targets for cancer therapy. Cancer gene therapy. 2005; 12(8):665–72. [PubMed: 15803146]
46. Julien SG, Dube N, Hardy S, Tremblay ML. Inside the human cancer tyrosine phosphatome. Nature reviews Cancer. 2011; 11(1):35–49. [PubMed: 21179176]
47. Chagnon MJ, Uetani N, Tremblay ML. Functional significance of the LAR receptor protein tyrosine phosphatase family in development and diseases. Biochemistry and cell biology = Biochimie et biologie cellulaire. 2004; 82(6):664–75. [PubMed: 15674434]
48. Davies M, Thomas GJ, Shewring LD, Mason RM. Mesangial cell proteoglycans: synthesis and metabolism. Journal of the American Society of Nephrology: JASN. 1992; 2(10 Suppl):S88–94. [PubMed: 1600141]
49. Bienkowski MJ, Conrad HE. Kinetics of proteoheparan sulfate synthesis, secretion, endocytosis, and catabolism by a hepatocyte cell line. The Journal of biological chemistry. 1984; 259(21): 12989–96. [PubMed: 6238032]
50. Owens RT, Wagner WD. Metabolism and turnover of cell surface-associated heparan sulfate proteoglycan and chondroitin sulfate proteoglycan in normal and cholesterol-enriched macrophages. Arteriosclerosis and thrombosis: a journal of vascular biology/American Heart Association. 1991; 11(6):1752–8.
51. Fedarko NS, Termine JD, Young MF, Robey PG. Temporal regulation of hyaluronan and proteoglycan metabolism by human bone cells in vitro. The Journal of biological chemistry. 1990; 265(21):12200–9. [PubMed: 2373688]

52. Zhang ZY. Protein tyrosine phosphatases: structure and function, substrate specificity, and inhibitor development. Annual review of pharmacology and toxicology. 2002; 42:209–34.

53. Skolnick J, Gao M. Interplay of physics and evolution in the likely origin of protein biochemical function. Proceedings of the National Academy of Sciences of the United States of America. 2013; 110(23):9344–9. [PubMed: 23690621]

54. Skolnick J, Gao M, Roy A, Srinivasan B, Zhou H. Implications of the small number of distinct ligand binding pockets in proteins for drug discovery, evolution and biochemical function. Bioorganic & medicinal chemistry letters. 2015; 25(6):1163–70. [PubMed: 25690787]

Summary Statement

This work reports novel sugar hydrolase and diesterase enzymatic activities in the phosphatase domain (PD) of PTPRδ in addition to monoester hydrolysis. Discovery of diverse enzymatic activities in the same protein domain has tremendous implications for understanding enzyme evolution.

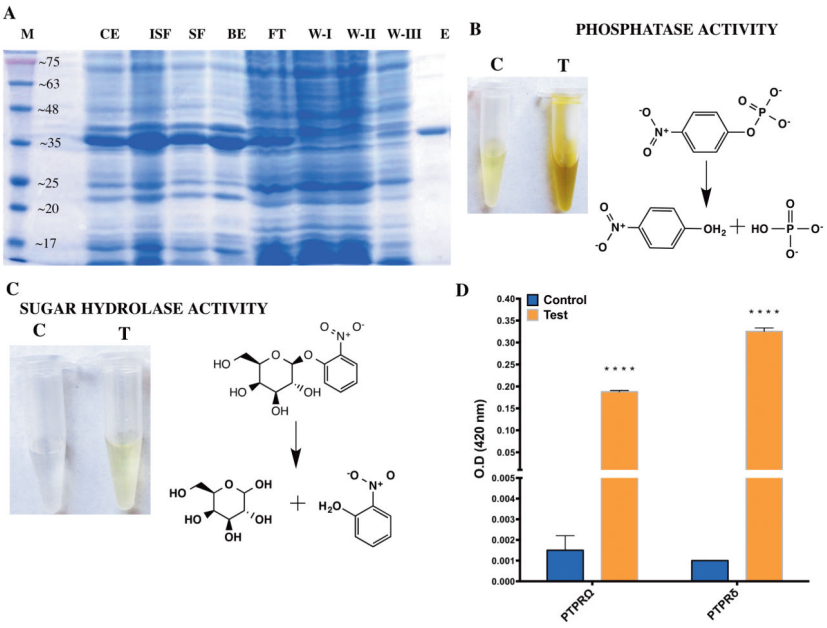

Fig. 1.

Protein purification and activity screen **(A)** Expression and purification profile of the phosphatase domain of Protein Tyrosine Phosphatae delta (PTPRδ). The protein was purified to homogeneity using IMAC purification. The gel image shows the systematic purification of the recombinantly expressed protein from proteins in the *E. coli* cell lysate. M: Molecular weight marker; CE: post-induction crude extract; ISF: in-soluble fraction; SF: soluble fraction; BE: Ni-NTA Beads; FT: Flow-through; W-I,II,III: Wash I, II and III, respectively. The numbers on the marker lane (M) indicates the molecular mass of the protein in KDa. **(B)** Assessment of phosphatase activity for the phosphatase domain of PTPRδ. The substrate employed is p-nitrophenyl phosphate and the reaction was allowed to proceed for 18 min at 37°C. **(C)** Assessment of sugar hydrolase activity for the phosphatase domain of PTPRδ. The substrate employed is o-nitrophenyl phosphate and the picture shows the reaction after 18 hours of incubation at 37°C. **(D)** hydrolysis of galactoside bond by PD-PTPRδ and PD-PTPRΩ as assessed on ONPG. Two way ANOVA was carried out to assess whether the difference was significant. A P-value of <0.0001 is represented by 4 “*” symbols. Notations “C” and “T” indicate control (without enzyme) and test (with enzyme), respectively and the reaction schemes were rendered with ChemBioDraw 14.0.

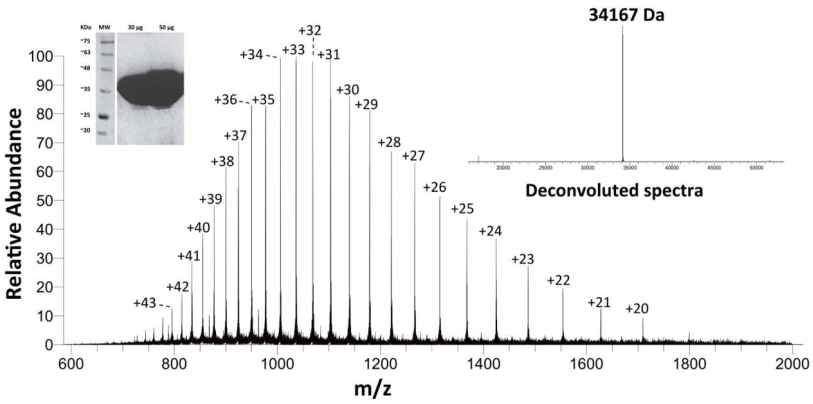

Fig. 2.

Mass spectrometric analysis of PD-PTPRδ. The mass spectra depicts the isotope clusters of the various charged states for the intact protein obtained by direct infusion of the protein into a high-mass accuracy Q-exactive Plus mass spectrometer. The right and left insets depict the deconvoluted spectra and the SDS-PAGE analysis with overloaded protein, respectively, as a means of assessing protein purity.

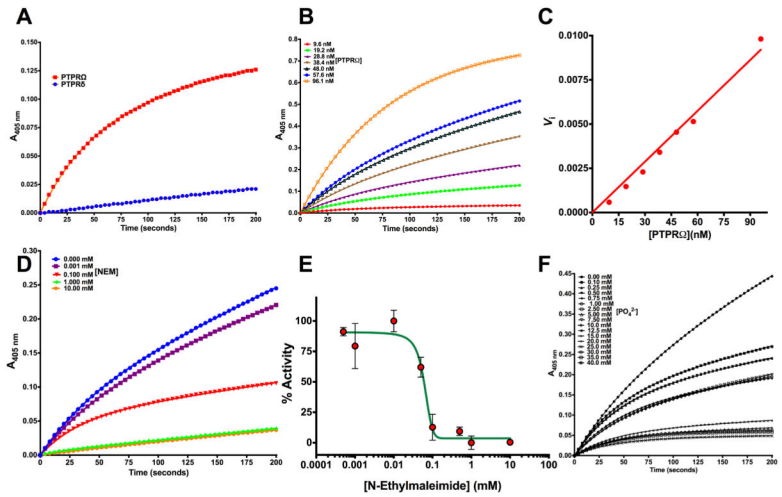

Fig. 3.

Hydrolysis of a phosphate substrate by PD-PTPRδ and PD-PTPRΩ **(A)** The time dependence of activity for PD-PTPRδ and PD-PTPRΩ. **(B)** Enzyme concentration dependence of the burst phase magnitude for PD-PTPRΩ as visualized on the time course measurement of substrate to product conversion. **(C)** Replot of data from (B) as a function of PD-PTPRΩ concentration. **(D)** Time course measurement of PD-PTPRΩ activity as a function of NEM concentration, an irreversible inhibitor, showing vanishing burst-phase. **(E)** Replot of % activity as a function of NEM concentration. **(F)** Time course measurement of PD-PTPRΩ activity as a function of phosphate concentration, a non-covalent reversible inhibitor, showing the retention of burst-phase. The symbols represent experimental data points, and the line represents the non-linear least squares fit. The Y-axis on panels (A, B, D and F) shows the optical density measurements estimated at 405 nm for the conversion of p-nitrophenyl phosphate to p-nitrophenol. The experimental data points were fit to the respective equations using the non-linear curve-fitting algorithm of GraphPad Prism v 6.0e or the software provided with Hitachi U-2010 UV-Vis spectrophotometer.

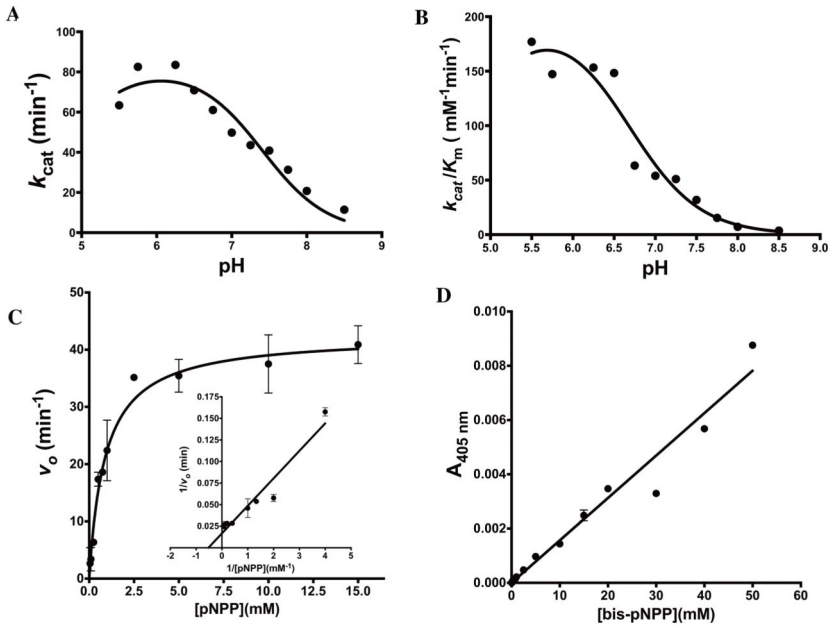

Fig. 4.

Characterization of phosphatase activity for PD-PTPRδ **(A)** Plot of k_{cat} as a function of pH **(B)** Plot of k_{cat}/K_m as a function of pH **(C)** Substrate vs. velocity plot for PD-PTPRδ hydrolysis of p-nitrophenyl phosphate showing hyperbolic kinetics. Inset shows the double-reciprocal Lineweaver-Burk plot. **(D)** Substrate vs. velocity plot for PD-PTPRδ hydrolysis of bis-p-nitrophenyl phosphate showing non-saturating kinetics even at the high concentration of 50 mM bis-pNPP. The experimental data points were fit to their respective equations using the non-linear curve-fitting algorithm of GraphPad Prism v 6.0e.

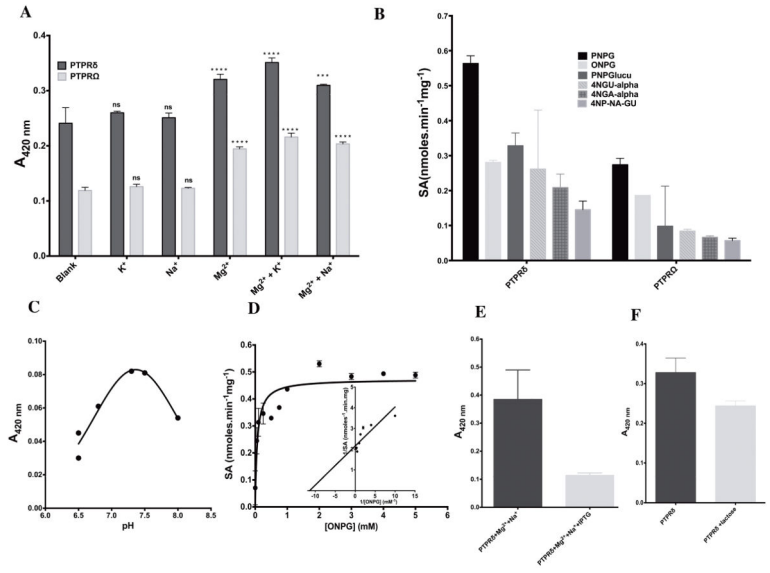

Fig. 5.

Characterization of sugar hydrolase activity for PD-PTPRδ and PD-PTPRΩ **(A)** Metal-ion dependence for sugar hydrolase activity of PD-PTPRδ and PD-PTPRΩ. The pairwise two-way ANOVA was performed between the blank and the respective test pairs. 4 "*" represents a P-value of <0.0001. **(B)** Screening of various sugar substrates to determine substrate discrimination across the PD-PTPRδ and PD-PTPRΩ. PNPG, p-nitrophenyl β-galactoside; ONPG, O-nitrophenyl β-galactopyranoside; PNPGlucu, p-nitrophenyl β-glucuronide; 4NGU-alpha, p-nitrophenyl α-D-glucoside; 4NGA-alpha, p-nitrophenyl α-D-galactoside; 4NP-NA-GU, p-nitrophenyl N-acetyl-β-D glucosaminide. **(C)** pH dependence for sugar hydrolase activity of PD-PTPRδ as assessed for ONPG **(D)** Substrate vs. velocity plot for PD-PTPRδ hydrolysis of o-nitrophenyl galactoside showing hyperbolic kinetics. Inset shows the double-reciprocal Lineweaver-Burk plot. **(E)** Effect of IPTG and **(F)** lactose on the sugar hydrolysis activity of PD-PTPRδ. The experimental data points were fit to the respective equations using the linear and nonlinear curve-fitting algorithm of GraphPad Prism v 6.0e.

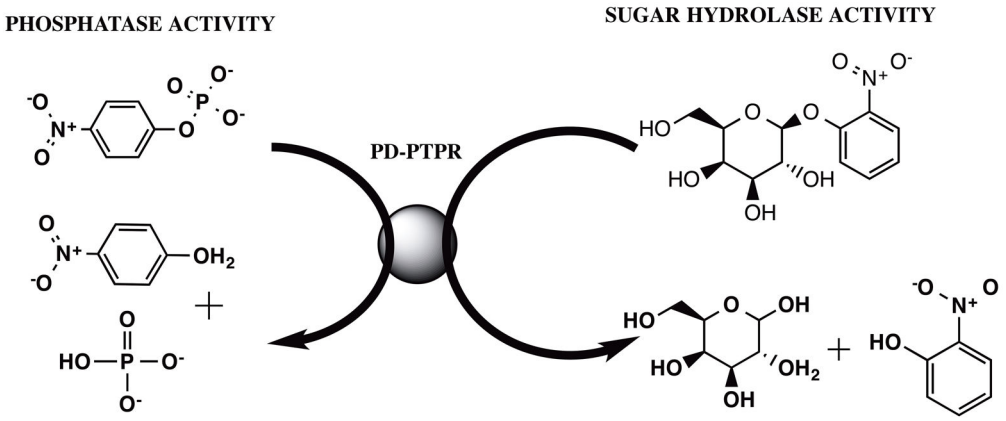

FACTORS	PHOSPHATASE	SUGAR HYDROLASE
CHEMISTRY	COP BOND CLEAVAGE	COC BOND CLEAVAGE
RATE ENHANCEMENT	~10^{17}	~10^{9}
DIVALENT/MONOVALENT METAL ION	NO EFFECT	ACTIVATOR METAL-DEPENDENT ACTIVITY
pH OPTIMA	6.3	7.3
IPTG	NO EFFECT	INHIBITOR
PHOSPHATE	INHIBITOR	NO EFFECT

Fig. 6.

Salient differences between the phosphatase and sugar hydrolase activity of PD-PTPRδ and PD-PTPRΩ. IPTG stands for isopropyl- β-D-1-thiogalactopyranoside and rate enhancement refers to the increase in the rate of a reaction vis-à-vis the uncatalyzed rate. The structure files were downloaded from PubChem and the figure was rendered with ChemBioDraw 14.0.

Table 1

Substrate screen for PD-PTPRδ and PD-PTPRΩ[1]

Bond Type		Substrate	PD-PTPRδ	PD-PTPRΩ
ester	monoester	p-nitrophenyl phosphate *, $	Yes	Yes
		Paraoxon$	No	No
		Mioticol$	No	No
		o-phospho tyrosine *	Yes	Yes
		adenosine monophosphate *	No	No
		inosine monophosphate *	No	No
		guanosine monophosphate *	No	No
		Pyridoxal 5′-phosphate *	No	No
	diester	Bis(p-nitrophenyl) phosphate $	Yes	Yes
		Tris (p-nitrophenyl) phosphate	No	No
		Tris (p-nitrobenzyl) phosphate	No	No
		Tetrakis (p-nitrophenyl) diphosphate	No	No
		nicotinamide adenine dinucleotide phosphate *	No	No
glycosidic		o-nitrophenyl β-D-galactoside#	Yes	Yes
		p-nitrophenyl β-D-galactoside#	Yes	Yes
		p-nitrophenyl β-D-glucuronide#	Yes	Yes
		p-nitrophenyl α-D-glucoside#	Yes	Yes
		p-nitrophenyl α-D-galactoside#	Yes	Yes
		p-nitrophenyl N-acetyl-β-D-glucosaminide#	Yes	Yes
peptide		H-Gly-PNA	No	No

*Chen's assay for liberated phosphate. The assay conditions were 100 mM Hepes pH 7.3, 20 mM $MgCl_2$, 20 mM of IMP, AMP, GMP and pNPP, 10 mM of PLP and 5 mM NADP, in 100 ul reaction mix. The assay was incubated for 30 min, quenched with 70 % TCA and the reaction mixture was added to Chen's reagent for color development and O.D readings were taken at 820 nm.

$Continuous assay for pNPP and bis-pNPP hydrolysis at 405 nm.

#End point assay for ONPG hydrolysis measurements at 420 nm.

[1]"Yes" indicates significant increase of activity in the test (+ enzyme) with respect to the control reaction (− enzyme) as assayed calorimetrically in an end point assay or a continuous assay.

"No" indicates no significant difference in the test activity (with enzyme) with respect to the control reaction (no enzyme). Significance was assessed by performing a t-test.

Table 2

Summary of kinetic parameters of PD-PTPRδ and PD-PTPRΩ for various substrates

Substrate	Enzyme/s	K_m (mM)	V_{max} (nmol min^{-1} mg^{-1})	k_{cat} (min^{-1})	k_{cat}/K_m ($mM^{-1}min^{-1}$)	Rate enhancement[1]
pNPP	PD-PTPRδ	0.64 ± 0.1	154 ± 6	1.6	2.44	~10^{17}
	PD-PTPRΩ (ss)	1.04 ± 0.3	3124 ± 243	2.0	1.92	~10^{17}
	PD-PTPRΩ (bp)	1.56 ± 0.3	9330 ± 666	7.6	4.87	~10^{17}
Bis-pNPP[2]	PD-PTPRδ[4]	NA	NA	NA	NA	NA
	PD-PTPRΩ(ss)	37.0 ± 4.7	10.96 ± 0.68	12.4	3.3×10^{-1}	~10^{9}
oNPG[3]	PD-PTPRδ	0.06 ± 0.01	0.47 ± 0.02	8.3×10^{-6}	1.4×10^{-4}	~10^{8}
p-Tyr[5]	PD-PTPRδ	NA	NA	NA	NA	NA

[1] Rate enhancement with respect to uncatalyzed reaction.

[2] The rate for spontaneous uncatalyzed cleavage rates of diester bonds are 1×10^{-10} sec. The value was obtained from Sasi *et al.,* (2014) Int. J. Chem. Mol. Nucl Mate. Metallur. Eng. 8(9), 1010–1012.

[3] The rate for spontaneous uncatalyzed cleavage rates of glycosidic bonds in adenosine were obtained from Stockbride *et al.,* (2010) Biorg Chem. 38(5), 224–228 and are reported by comparing them with the sugar bond hydrolysis rates in our study. It should be pointed out that conventional glycoside hydrolases produce a rate enhancement of ~10^{12}.

[4] The fits were unreliable with very wide confidence intervals given that the curve was not saturating (Fig 4D)

[5] The fits were unreliable with very wide confidence intervals given that the curve was not saturating (Fig S2C)